Abdul-Khaalig Mohamed*, Vered Aharonson

Bayesian input model selection for wrist control by a bionic hand

https://doi.org/10.1515/cdbme-2025-0204

Abstract: Dynamic causal modelling is a promising tool to quantify hand movement neural control. It portrays the temporal path of signals across a network of distinct motor control areas in the brain. Optimising the input representation for this modelling framework—including defining the input signal and its entry point into the motor-control network could enhance its ability to explain interactions within the brain. A more precise characterisation of these inputs may also shed light on visuomotor coordination, which is linked to efficient brain-computer interface usage and bionic hand control. This study applied Bayesian selection to determine the optimal input model. Electroencephalography recordings were acquired from three participants who performed wrist extension and wrist flexion movements. Nine candidate input models were compared using the Bayesian selection's logevidence. The selection was evaluated by the spectral variance between each participant's measured spectrograms and those predicted by the winning model. In all participants, the same input model was selected: an input signal of three gamma functions entering the left and right premotor cortices. This input model provides insights into visuomotor coordination and can improve the performance of a brain-computer interface controlling a bionic hand.

Keywords: brain-computer interface, dynamic causal modelling, Bayesian model selection, EEG, wrist extension, wrist flexion

1 Introduction

Bionic prosthetic and orthotic hands could assist motorimpaired individuals in performing daily living activities [1]. This technology uses sensorimotor brain-computer interfaces (BCI) to interpret the person's hand-movement intention from recorded electroencephalography (EEG) signals [1]. Low spatial resolution, noise contamination, and their inherent spatial and temporal complexity, hamper EEG signals' interpretation [2], and 15–30% of users are unable to generate sensorimotor brain signals for BCI control [3].

Dynamic causal modelling of induced responses (DCM-IR) is a leading EEG analysis framework [4] that estimates the time-frequency response to experimental events through causal, cross-frequency couplings between multiple brain regions [5,6]. The modelling entails a set of differential equations (eq 1), where the hidden states $g(\omega,t)$ —functions of frequency (ω) and time (t)—are the neural response in the brain regions participating in the movement control [7].

$$\tau \dot{g}(\omega, t) = (A + XB)g(\omega, t) + \mathcal{C}u(t) \tag{1}$$

The parameters of Matrix A and Matrix B respectively model couplings between the regions without, and due to, changes in exogenous experimental conditions [8]. The second term in the equation is the input model. It consists of an input signal, u(t), and a binary vector, C, which represents the primary motor regions that receive the input signal [8]. In experiments and BCI training sessions involving visual neurofeedback, an accurate representation of the input model could explain communication between the visual cortex and the network of motor cortices. This could elucidate visuomotor co-ordination, which has been linked to BCIinefficiency [3].

Previous EEG DCM-IR studies of hand movement indicated that the input regions are the supplementary motor cortex (SMA), the premotor cortex (PMv), or the prefrontal cortex (PFC); and that the signal u(t) can be represented by either a single input gamma function [6,9–11] or two gamma functions [12]. No previous study performed a selection

^{*}Corresponding author: Abdul-Khaaliq Mohamed, School of Electrical and Information Engineering, University of the Witwatersrand, Johannesburg, 1 Jan Smuts ave, Braamfontein 2000, ZA. e-mail: abdul-khaaliq.mohamed@wits.ac.za Vered Aharonson: School of Electrical and Information Engineering, University of the Witwatersrand, Johannesburg, 1 Jan Smuts ave, Braamfontein 2000, ZA and Medical School, University of Nicosia, 93 Agiou Nikolaou Street, Engomi 2408, CY.

process to determine the optimal entry regions and the optimal number of gamma functions in u(t).

Our study employed Bayesian model selection (BMS) to optimise the DCM-IR input model for two experimental conditions: wrist extension and wrist flexion movements.

2 Method

Three bilateral fully-connected DCM-IR architectures, illustrated in Figure 1, were developed based on empirical and physiological wrist-control data from the literature. All architectures included seven cortical regions, listed in Table 1 [6,9,11,12], and differed in their input entry model. For each entry model, three potential input signals, shown in Figure 2, were considered; resulting in a total of nine possible input models. The input signals were composed of one, two or three gamma functions—time-linked to the visual cues of the experiments' wrist motor tasks [12,13]. Coupling parameter estimation was conducted for all plausible models. A winning input model was thereafter computed using Bayesian model selection (BMS).

The details of the instrumentation and EEG data acquisition were reported elsewhere [13]. A preliminary cohort of one male and two female participants, screened and shown to be BCI-efficient [14], performed wrist extension and wrist flexion movements. Wrist movements were controlled by the IsoReg dynamometer [13] that regulated force, speed and range deviations. Each participant performed 100 trials of wrist extensions and 100 wrist flexions [13]. The EEG data was recorded using a 128-channel Brain Products actiCHamp system (Brain Products GmbH, Gilching, Germany). The single-trial EEG data were pre-processed using Matlab 2019b (The Mathworks Inc, Natick, MA, USA) and EEGLAB [15] to estimate distinct signals from the seven brain regions through inverse lead-field matrix source localisation [6].

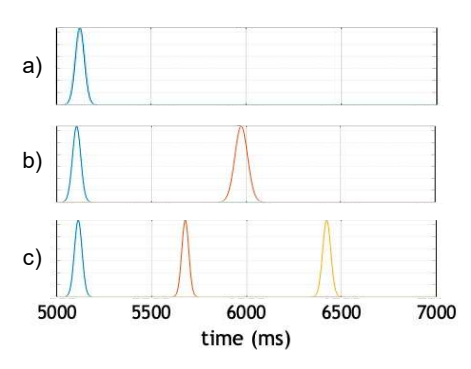


Figure 2: Time plots of exogenous inputs u(t) with a) one, b) two and c) three gamma functions. Visual cues to prepare to move, and to sustain the wrist movement, were displayed at t=5000, and t=0 ms respectively.

Table 1: The seven regions in the dynamic causal model architectures and their anatomical descriptions.

Region Abbreviation	Anatomical region name
r-M1-H; I-M1-H	Right- and left-hand representation in the Primary motor cortex
SMA	Supplementary motor area
r-PMv; I-PMv	Right and left ventral pre-motor cortex
r-PFC; I-PFC	Right and left prefrontal cortex

Morlet wavelet transform [7] provided the time-frequency spectrograms of the measured pre-processed signals—per brain region, participant and trial. Spectrogram windows were 5000–7000 ms peristimulus time, and covered a frequency range of 1 to 90 Hz [13]. The spectrograms were then averaged across all trials for each brain region and each movement type [16]. Spectrogram generation, parameter optimisation, and model selection were implemented using the Statistical Parametric Mapping software revision 12 (Wellcome-Trust Centre for Neuroimaging, London, UK).

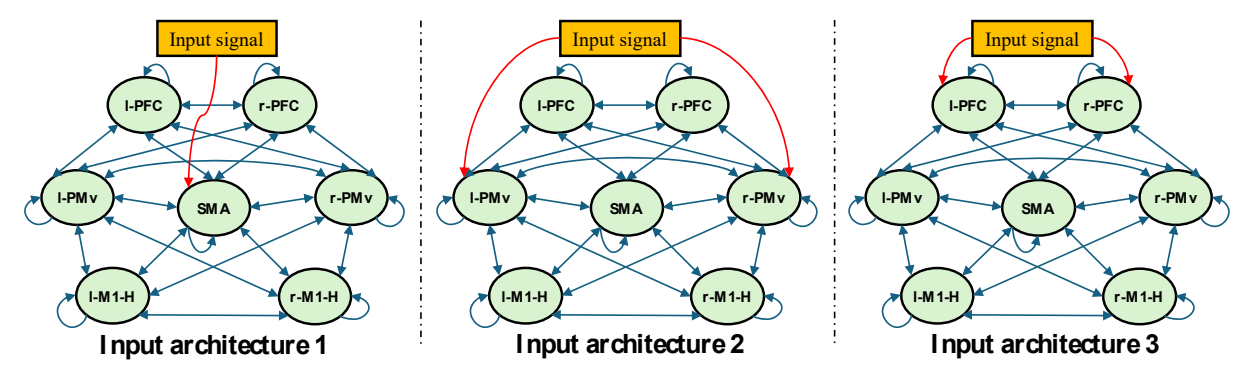


Figure 1: Three plausible candidate DCM input architectures based on physiology from literature. Red arrows depict the input signal origin and blue arrows depict region connections. Abbreviations for the brain regions (in green) are defined in Table 1.

Bayesian inversion parameter optimisation minimised the difference between the spectrograms predicted by the DCM-IR— $g(\omega,t)$ in eq (1)—and the measured spectrograms, using the Expectation-Maximisation algorithm and a log-evidence objective function [8]. Fixed-effects BMS [7] computed the log evidence of the nine candidate models for each participant and selected the model with the highest log evidence. Random-effects BMS [7] determined the best model across the cohort of three participants. Model selection performance was evaluated using the spectral variance (R^2) [6] between each participant's measured spectrograms and those predicted by the winning model. Additionally, a visual comparison between the measured and predicted spectrograms was performed to complement the quantitative evaluation.

3 Results

Figure 3a shows the fixed-effects BMS log-evidence values of the nine models for participants 1, 2, and 3. The models are denoted by the entry model and input number of gamma functions. For example, model 1-1 uses input entry 1 (Figure 1) and one gamma function in u(t). Model 2-3 yielded the highest log evidence. This input model consists of a three-gamma-functions input entering the brain regions network from right and left ventral pre-motor cortex. The random-effects BMS in Figure 3b shows the prominence of model 2-3 for the 3-participant cohort.

The R^2 values for model 2-3 were 74.76%, 90.00% and 83.56% for participants 1, 2 and 3 respectively. Figure 4 depicts an example of all measured and predicted spectrograms of participant 1, showing the similarity of the spectrograms.

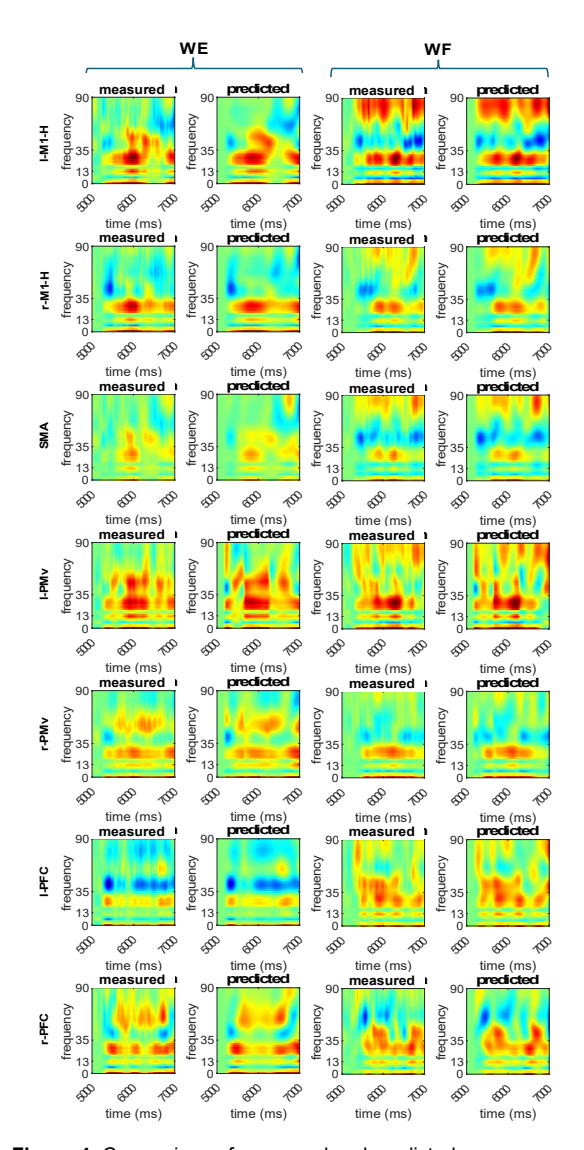


Figure 4: Comparison of measured and predicted spectrograms—for model 2-3 and for the RH of participant 1. Abbreviations for the brain regions are defined in Table 1.

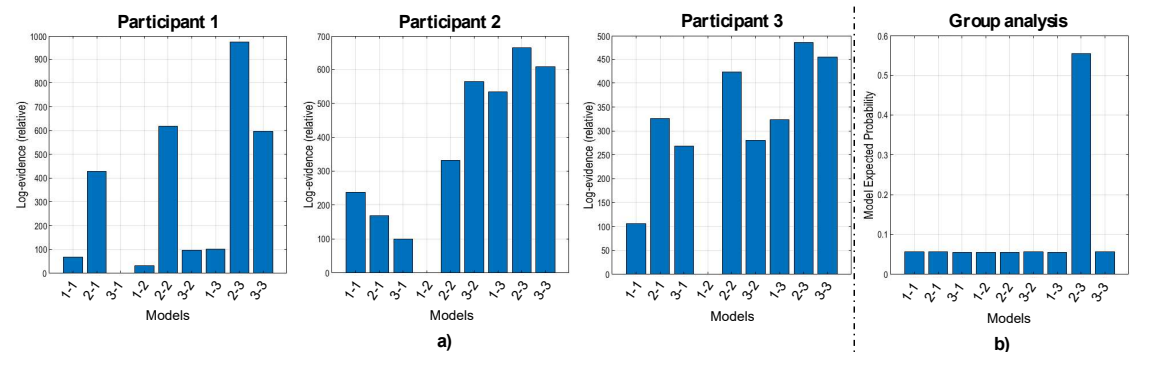


Figure 3: a) Participant-specific results of BMS using fixed effects. Model 1-1 is labelled according to using architecture 1 and using one gamma function for *u*(*t*). The other eight models are similarly labelled. b) Group results for BMS using random effects.

4 Discussion and Conclusion

This study proposes an input-model selection framework for dynamic causal modelling of visuomotor control in wrist extension and wrist flexion. These movements are pivotal for effectively controlling a bionic hand [1]. The findings presented are preliminary, as EEG data from only three participants were used to establish ground-truth spectrograms for the models' predictions. However, the consistency of the selected model across all three participants suggests its potential applicability to broader populations. This hypothesis will be tested and validated on a larger cohort. The selected input model includes three sequential gamma functions entering the left and right premotor cortices. This model provides insight into visuomotor coordination, which was previously linked with BCI inefficiency [3]. It thus represents a step towards explaining wrist-extension and wrist-flexion visuomotor control using a BCI.

In our present study, evaluation of the model fit was limited to R², since DCM-IR produces trial-averaged spectra and cannot label unseen single-trial data [6]. Moreover, the current sample is too small for a robust generalisation estimate. Classification accuracy will therefore be examined in a subsequent investigation, with an expanded sample, and a discriminative decoder that couples the optimised input model with BCI classification methods from our previous study [14].

Author Statement

This research was funded by the National Research Foundation of South Africa, grant numbers 99207 and 117965. Authors state no conflict of interest. Informed consent has been obtained from all individuals included in this study. The research complies with all the relevant national regulations, institutional policies, and was performed in accordance with the tenets of the Helsinki Declaration. It has been approved by Medical Human Research Ethics Committee at the University of Witwatersrand (clearance certificate number M190607, July 2019).

References

- [1] Abiri, R.; Borhani, S.; Sellers, E.W.; Jiang, Y.; Zhao, X. A Comprehensive Review of EEG-Based Brain–Computer Interface Paradigms. J. Neural Eng. 2019, 16, 011001.
- [2] Hamedi, M.; Salleh, S.-H.; Noor, A.M. Electroencephalographic Motor Imagery Brain Connectivity Analysis for BCI: A Review. *Neural Comput.* 2016, 28, 999– 1041.
- [3] Lee, M.; Yoon, J.-G.; Lee, S.-W. Predicting Motor Imagery Performance From Resting-State EEG Using Dynamic Causal Modeling. Front. Hum. Neurosci. 2020, 14, 321.

- [4] Friston, K.J.; Preller, K.H.; Mathys, C.; Cagnan, H.; Heinzle, J.; Razi, A.; Zeidman, P. Dynamic Causal Modelling Revisited. *NeuroImage* 2019, 199, 730–744.
- [5] Chen, C.-C.; Kilner, J.M.; Friston, K.J.; Kiebel, S.J.; Jolly, R.K.; Ward, N.S. Nonlinear Coupling in the Human Motor System. *J. Neurosci.* 2010, *30*, 8393–8399.
- [6] Wilkins, K.B.; Yao, J. Coordination of Multiple Joints Increases Bilateral Connectivity with Ipsilateral Sensorimotor Cortices. *NeuroImage* 2020, 207, 116344.
- [7] Stephan, K.E.; Penny, W.D.; Moran, R.J.; den Ouden, H.E.M.; Daunizeau, J.; Friston, K.J. Ten Simple Rules for Dynamic Causal Modeling. *NeuroImage* 2010, 49, 3099– 3109
- [8] Chen, C.C.; Kiebel, S.J.; Friston, K.J. Dynamic Causal Modelling of Induced Responses. *NeuroImage* 2008, 41, 1293–1312.
- [9] Larsen, L.H.; Zibrandtsen, I.C.; Wienecke, T.; Kjaer, T.W.; Langberg, H.; Nielsen, J.B.; Christensen, M.S. Modulation of Task-Related Cortical Connectivity in the Acute and Subacute Phase after Stroke. *Eur. J. Neurosci.* 2018, 47, 1024–1032.
- [10] Nettersheim, F.S.; Loehrer, P.A.; Weber, I.; Jung, F.; Dembek, T.A.; Pelzer, E.A.; Dafsari, H.S.; Huber, C.A.; Tittgemeyer, M.; Timmermann, L. Dopamine Substitution Alters Effective Connectivity of Cortical Prefrontal, Premotor, and Motor Regions during Complex Bimanual Finger Movements in Parkinson's Disease. *NeuroImage* 2019, *190*, 118–132.
- [11] Herz, D.M.; Christensen, M.S.; Reck, C.; Florin, E.; Barbe, M.T.; Stahlhut, C.; Pauls, K.A.M.; Tittgemeyer, M.; Siebner, H.R.; Timmermann, L. Task-Specific Modulation of Effective Connectivity during Two Simple Unimanual Motor Tasks: A 122-Channel EEG Study. NeuroImage 2012, 59, 3187–3193.
- [12] Bönstrup, M.; Schulz, R.; Feldheim, J.; Hummel, F.C.; Gerloff, C. Dynamic Causal Modelling of EEG and fMRI to Characterize Network Architectures in a Simple Motor Task. *NeuroImage* 2016, 124, 498–508.
- [13] Mohamed, A.-K.; Aswat, M.; Aharonson, V. Low-Cost Dynamometer for Measuring and Regulating Wrist Extension and Flexion Motor Tasks in Electroencephalography Experiments. Sensors 2024, 24, 5801.
- [14] Mohamed, A.-K.; Aharonson, V. Single-Trial Electroencephalography Discrimination of Real, Regulated, Isometric Wrist Extension and Wrist Flexion. *Biomimetics* 2025, 10, 187
- [15] Delorme, A.; Makeig, S. EEGLAB: An Open Source Toolbox for Analysis of Single-Trial EEG Dynamics Including Independent Component Analysis. *J. Neurosci. Methods* 2004, 134, 9–21.
- [16] Chen, C.-C.; Kiebel, S.J.; Kilner, J.M.; Ward, N.S.; Stephan, K.E.; Wang, W.-J.; Friston, K.J. A Dynamic Causal Model for Evoked and Induced Responses. *NeuroImage* 2012, 59, 340–348.